Int. J. Heat Mass Transfer. Vol. 17, pp. 11–21. Pergamon Press 1974. Printed in Great Britain

CONVECTIVE EFFECTS IN ENCLOSED, EXOTHERMICALLY REACTING GASES

D. R. JONES

School of Mathematics and Physics, University of East Anglia, Norwich, England*

(*Received* 18 *December* 1972 *and in revised form* 12 *June* 1973)

Abstract—The consequences of the occurrence of convection when exothermic chemical reactions take place in a gaseous medium enclosed in a horizontal circular cylinder are investigated by means of a numerical integration of the governing fluid-dynamical equations using an A.D.I. technique. The thermal effects of the reaction are represented by a distribution of heat sources with an Arrhenian temperature dependence but the consumption of reactants during the reaction is ignored. The ignition limit δ_{CR} is found to be a strongly increasing function of the Rayleigh number and the temperature distributions in the vessel are no longer symmetrical about the centre when convection occurs. Good qualitative agreement with the observations of convective effects in experiments using vessels of other geometries is obtained.

NOMENCLATURE

A, pre-exponential factor in Arrhenius' law;
E, activation energy of reaction;
g, acceleration due to gravity;
l, radius of cylindrical vessel;
p, dimensionless pressure;
Pr, Prandtl number, ν/κ;
Q, exothermicity of reaction;
r, θ, dimensionless polar co-ordinates;
R, gas constant;
Ra, Rayleigh number;
T, temperature;
$\boldsymbol{u}$, dimensionless velocity;
$\hat{\boldsymbol{z}}$, unit vector in vertical direction.

Greek symbols

α, coefficient of cubical expansion of reacting gas;
β, RT_0/E;
δ, $QEAl^2 \exp(-E/RT_0)/\kappa RT_0^2$;
δ_{CR}, critical value of δ for onset of explosion;
κ, thermal diffusivity of reacting gas;
ν, kinematic viscosity of reacting gas;
ρ, density of reacting gas;
ϕ, dimensionless temperature;
ψ, dimensionless stream function;
ω, dimensionless vorticity.

Subscripts

i, j, n, value at ith grid point in r-direction and jth in θ-direction at the nth time-step;
0, value at wall of vessel.

Superscripts

(s), denotes sth iterate.

1. INTRODUCTION

THE CLASSICAL theory of thermal ignition developed by Frank-Kamenetskii [1] describes exothermically reacting systems in which the heat transfer mechanism is purely conductive. Steady-state regimes in vessels of three different geometries are discussed in [1]. The three cases are those in which the reacting medium is confined (i) between two infinite horizontal plates, (ii) inside a horizontal circular cylinder, and (iii) inside a sphere. Although later authors [2, 3] have been able to improve upon and extend the basic theory and, using numerical techniques, to retain the time-dependence of the model, which Frank-Kamenetskii was forced to relinquish, all have continued to assume that heat transfer takes place by conduction alone. However, of the temperature distributions predicted in [1], which are in each case symmetrical about the centre of the vessel, only that for the case (i) can exist in equilibrium if the reacting medium is a fluid, since those for the cylindrical and spherical cases imply the existence of temperature gradients perpendicular to the direction of the gravity vector. In these cases convection should be expected to occur.

Experimental evidence of convective effects has been reported by several authors. Tyler [4] and Ashmore, Tyler and Wesley [5] observed asymmetries in the temperature distributions in reacting systems contained in spherical vessels, with the maxima occurring significantly above, rather than at, the

* Present address: Building Research Station, Garston, Watford, England.

centre of the vessel for sufficiently large values of the Rayleigh number. This is the dimensionless parameter characterizing the relative importance of conduction and convection processes. Using a parallel-plate vessel, Merzhanov and Shtessel [6] monitored the increase with the Rayleigh number of the critical value δ_{CR} of Frank-Kamenetskii's parameter δ dividing explosive regimes ($\delta > \delta_{CR}$) from steady-state regimes ($\delta < \delta_{CR}$). The parameter δ is a measure of the ratio of the rate of heat production by the chemical reaction and the rate at which heat is conducted through the reacting medium. Ultimately, whether or not the system explodes is determined by the balance between the rate of production of heat by the reaction and the rate of removal of heat from the system by conduction through the walls of the enclosing vessel. The increase of the critical value of δ with the Rayleigh number observed in [6] is due to the enhancement of the transfer of heat through the reacting medium to the walls when convection occurs in addition to conduction, thus allowing a higher rate of heat production to be accommodated without an explosion.

The purely conductive theories of [1–3] are governed by the diffusion equation for the temperature field, with an internal heat source term whose temperature dependence is given by Arrhenius' law to represent the thermal effects of the reaction. Here, further terms describing the convective heat transfer processes are incorporated, so that two more equations, the continuity and momentum equations governing the velocity field, are required to complete the specification of the problem. No details of the chemical kinetics are included; the combustion reaction is assumed to be of zero order. Thus the consumption of reactants during the course of the reaction is ignored. The system of governing equations is considered in detail in Section 2. Jones [7] used these equations in estimating the lowest values of the Rayleigh number at which convective effects are likely to be significant in the parallel-plate vessel of case (i) by an examination of the stability of Frank-Kamenetskii's solutions to small perturbations of the temperature and velocity fields.

The importance of convection in the cylindrical case (ii) is investigated in this paper by a less restricted technique, namely the numerical integration of the full governing equations. A so-called 'split-operator' finite-difference method (essentially the alternating-direction implicit method of Peaceman and Rachford [8]) is employed to advance the solutions step-by-step in time from the imposed initial conditions. The motion of the reacting gas is assumed to be two-dimensional and the spatial finite-difference mesh is based on the natural polar co-ordinate system for the cylinder. The non-linearities of the governing equations are treated by means of iterative procedures at each time-step. A more detailed account of the numerical method is to be found in Section 3.

By performing the integration for several combinations of values of δ and the Rayleigh number Ra and observing the nature of the resulting solutions, that is whether the reaction proceeds to a steady-state or to an explosion, the dependence of the critical value δ_{CR} of the parameter δ on the Rayleigh number is delimited. It is found that δ_{CR} is a strongly increasing function of Ra. For example, a Rayleigh number of order 10^4, which is attainable in experimental systems, may lead to a 200–300 per cent increase in δ_{CR} compared with the value predicted by Frank-Kamenetskii's theory.

The maxima of the temperature distributions calculated here are displaced from the centre towards the top of the vessel, in agreement with the experimental observations of [4] and [5]. This displacement is associated with an upwelling of warm fluid near the centre of the vessel. In Section 4 the details of the results of the numerical integrations are presented and their relationship with the observations of experimental systems discussed.

2. THE GOVERNING EQUATIONS

In formulating the equations governing the dynamics and thermodynamics of the chemically reacting fluid system studied here, we represent the thermal effects of the reaction by a spatial distribution of heat sources within the fluid. Details of the chemical kinetics of the reaction are not taken into account. Further, variations of the concentrations of the reactants during the reaction, and their convective and diffusive motions are also ignored. As a first approximation it is reasonable to neglect the effects of reactant consumption since previous calculations (see, for example, [3]) suggest that frequently only of the order of 5 per cent of the reactants are consumed during the period in which the system reaches its maximum temperature. If the reaction has exothermicity Q, and if its rate is determined by a reaction step of activation energy E, then using Arrhenius' law for the temperature dependence of the reaction rate we find that the density q of heat sources to be included in the energy equation is given by

$$q = QA \exp(-E/RT), \tag{1}$$

where A is a constant, R is the gas constant and T is the temperature of the gas.

The inclusion in the energy equation of terms describing convective heat transfer processes requires the introduction of the momentum and continuity

equations for the fluid velocity in order to complete the system of governing equations. Here we assume that the reacting medium may be considered to be a Newtonian fluid whose motion is laminar. In deriving the governing equations we make the Boussinesq approximation in which the density ρ of the fluid depends on the temperature according to

$$\rho - \rho_0 = -\alpha\rho_0(T - T_0), \tag{2}$$

where α is the coefficient of cubical expansion of the fluid and $\rho_0 = \rho(T_0)$, in the buoyancy force term of the momentum equation, but the density and all other physical parameters of the fluid are assumed to be constant elsewhere. This approximation may be justified provided that the temperature T satisfies

$$|T - T_0| \ll T_0, \tag{3}$$

everywhere if T_0 is an absolute temperature typical of the system, here taken to be the wall temperature. If, further, we have

$$u^2/c^2 \ll |T - T_0|/T_0, \tag{4}$$

where u is a velocity typical of the convective motion of the reacting medium and c is the speed of sound within the medium, then the dissipation term in the energy equation may be neglected.

The governing equations derived in this way may be written in dimensionless form in the following manner. Distances are non-dimensionalised with respect to the radius l of the vessel, times are measured in units of l^2/κ, velocities in units of ν/l and the pressure in units of $\kappa\nu\rho_0/l^2$, where ν is the kinematic viscosity of the reacting medium and κ its thermal diffusivity. We adopt Frank-Kamenetskii's dimensionless temperature ϕ defined by

$$\phi = \frac{E}{RT_0^2}(T - T_0). \tag{5}$$

Then the continuity, momentum and energy equations may be written

$$\nabla . \boldsymbol{u} = 0, \tag{6}$$

$$\frac{\partial \boldsymbol{u}}{\partial t} + Pr(\boldsymbol{u} . \nabla)\boldsymbol{u} = -\nabla p + Pr\nabla^2\boldsymbol{u} + Ra\phi\hat{\boldsymbol{z}}, \tag{7}$$

and

$$\frac{\partial \phi}{\partial t} + Pr(\boldsymbol{u} . \nabla)\phi = \nabla^2\phi + \delta \exp\{\phi/(1 + \beta\phi)\}, \tag{8}$$

respectively, where $\boldsymbol{u}$ is the fluid velocity and $\hat{\boldsymbol{z}}$ is a unit vector in the vertical direction. The dimensionless parameters characterising the system are the Rayleigh number

$$Ra = gl^3\alpha RT_0^2/\kappa\nu E, \tag{9}$$

the Prandtl number

$$Pr = \nu/\kappa, \tag{10}$$

Frank-Kamenetskii's parameter

$$\delta = QEAl^2 \exp(-E/RT_0)/\kappa RT_0^2, \tag{11}$$

and

$$\beta = RT_0/E. \tag{12}$$

We shall take $\beta = 0$ throughout our calculations, although this is not necessitated by the method employed. Parks [9] has shown that the critical condition for explosion varies by at most about 5 per cent from its value for $\beta = 0$ when β is less than 0·05, values above which are not appropriate to gas-phase reactions.

The parabolic system of governing equations (6)–(8) is solved subject to initial conditions of the form

$$\phi = \phi_{\text{INIT}} \quad \text{and} \quad \boldsymbol{u} = \boldsymbol{u}_{\text{INIT}} \quad \text{at} \quad t = 0, \tag{13}$$

where ϕ_{INIT} and $\boldsymbol{u}_{\text{INIT}}$ are functions of position. The boundary condition imposed on the temperature of the reacting gas at the walls of the vessel is that it should remain equal to the temperature of the walls, that is

$$\phi = 0 \quad \text{on} \quad r = 1 \quad \text{for all} \quad t \geqslant 0. \tag{14}$$

The velocity field within the vessel is require to satisfy the usual condition for a viscous fluid at a solid wall, namely

$$\boldsymbol{u} = 0 \quad \text{on} \quad r = 1 \quad \text{for all} \quad t \geqslant 0. \tag{15}$$

3. THE NUMERICAL METHOD

In this Section we describe the finite-difference method used to obtain solutions of the governing equations (6)–(8), subject to the initial conditions (13) and the boundary conditions (14) and (15). The vessel geometry considered is the horizontal circular cylinder of case (ii) of Frank-Kamenetskii's work. We assume that the fluid motion is confined to vertical planes perpendicular to the axis of the cylinder, and that, in addition, this two-dimensional motion is symmetric about the vertical diameter. Hence solutions are sought in the semicircular region shown in Fig. 1. The natural (dimensionless) polar co-ordinates (r, θ) with origin at the centre of the vessel are employed.

It is convenient to introduce the stream function ψ satisfying

$$u_r = \frac{1}{r}\frac{\partial \psi}{\partial \theta} \quad \text{and} \quad u_\theta = -\frac{\partial \psi}{\partial r}, \tag{16}$$

where u_r and u_θ are the polar components of $\boldsymbol{u}$, so that the continuity equation (6) is identically satisfied. The

vorticity ω defined by

$$\omega = \nabla \times u, \tag{17}$$

has only one non-zero component, ω say, for the two-dimensional motions considered here, namely the

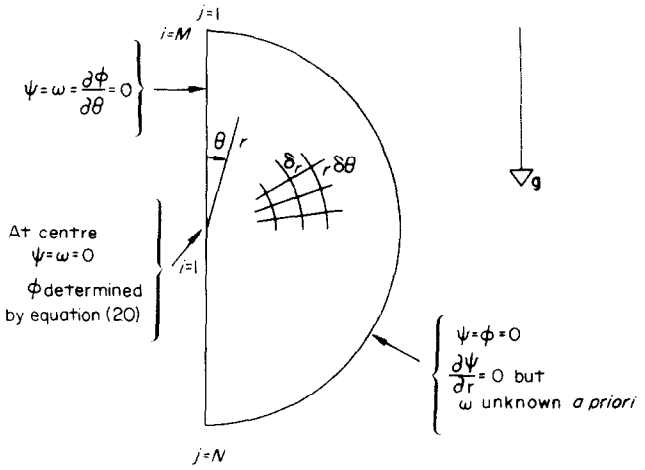

FIG. 1. The integration region.

component parallel to the axis of the cylinder. From (16) and (17) it follows that ψ and ω are related by

$$\frac{1}{r}\frac{\partial}{\partial r}\left(r\frac{\partial \psi}{\partial r}\right) + \frac{1}{r^2}\frac{\partial^2 \psi}{\partial \theta^2} = -\omega. \tag{18}$$

In terms of ψ and ω the remaining equations (7) and (8) may be written

$$\frac{\partial \omega}{\partial t} + \frac{Pr}{r}\left(\frac{\partial \omega}{\partial r}\frac{\partial \psi}{\partial \theta} - \frac{\partial \omega}{\partial \theta}\frac{\partial \psi}{\partial r}\right) = Pr\left[\frac{1}{r}\frac{\partial}{\partial r}\left(r\frac{\partial \omega}{\partial r}\right) + \frac{1}{r^2}\frac{\partial^2 \omega}{\partial \theta^2}\right] - Ra\left(\sin\theta\frac{\partial \phi}{\partial r} + \frac{\cos\theta}{r}\frac{\partial \phi}{\partial \theta}\right), \tag{19}$$

and

$$\frac{\partial \phi}{\partial t} + \frac{Pr}{r}\left(\frac{\partial \phi}{\partial r}\frac{\partial \psi}{\partial \theta} - \frac{\partial \phi}{\partial \theta}\frac{\partial \psi}{\partial r}\right) = \frac{1}{r}\frac{\partial}{\partial r}\left(r\frac{\partial \phi}{\partial r}\right) + \frac{1}{r^2}\frac{\partial^2 \phi}{\partial \theta^2} + \delta \exp\left[\phi/(1+\beta\phi)\right], \tag{20}$$

respectively, where the pressure has been eliminated by applying the operator $\nabla \times$ to equation (7).

The boundary condition (15) on the velocity field becomes

$$\psi = \text{constant}, \quad \frac{\partial \psi}{\partial r} = 0 \quad \text{on} \quad r = 1 \quad \text{for all} \quad t \geqslant 0, \tag{21}$$

and it is convenient to choose the constant in (21) to be zero. The assumption of symmetry about the vertical diameter leads to the conditions

$$\psi = \omega = 0, \tag{22}$$

and

$$\frac{\partial \phi}{\partial \theta} = 0, \tag{23}$$

on $\theta = 0, \pi$ for all $t \geqslant 0$.

Finite-difference methods are employed to obtain solutions of the governing equations in the form (18)–(20), subject to the boundary conditions (14) and (21)–(23), and a variety of initial conditions of the form (13). The non-linearity of the equations (19) and (20) necessitates the use at each time-step of an iterative technique, each stage of which involves the solution of linear problems only. The method is described in detail in the summary of the integration procedure set out below.

The spatial mesh chosen is illustrated in Fig. 1. It is that naturally suggested by the use of polar co-ordinates and allows the conditions at the outer boundary ($r = 1$) and on the line of symmetry ($\theta = 0, \pi$) to be incorporated conveniently into the solution scheme, although special consideration of the centre of the vessel ($r = 0$) is required.

At each stage of the iterative process, the alternating direction implicit (A.D.I.) method first proposed by Peaceman and Rachford [8] is employed in the solution of (19) and (20). In using this method, each time-step, $\Delta t = t_{n+1} - t_n$ say, is divided into two halves. For the first half time-step, in which the solutions are advanced from t_n to $t_{n+\frac{1}{2}}$ derivatives with respect to r are represented by finite-difference

analogues evaluated at $t_{n+\frac{1}{2}}$ whereas those with respect to θ are evaluated at t_n where the solutions are already known. In advancing from $t_{n+\frac{1}{2}}$ to t_{n+1} the procedure is reversed, with θ-derivatives evaluated at t_{n+1} but r-derivatives at $t_{n+\frac{1}{2}}$ where the values are known from the results of the first half time-step. Backward differences are utilised in the representation of the time derivatives at each half time-step and space derivatives are represented by central differences. This leads to a procedure which is, overall, unconditionally stable and has truncation errors of second order with respect to both the time and space mesh sizes. The principal advantage of such a method is, of course, that the matrix of coefficients which it yields at each half time-step is tridiagonal, and efficient algorithms exist for the solution of systems of this kind.

Although the set of boundary conditions (14) and (15) specified in the original statement of the problem under discussion is complete, the reformulation of the problem in terms of the stream function and vorticity, and the assumption of symmetry about the vertical diameter leave incomplete the set of conditions required on the boundary of the semicircular region in which the numerical integration is to be performed, as Fig. 1 shows. Two conditions, the vorticity at the solid outer boundary, and the temperature at the centre of the vessel, are not known *a priori* and must be determined during the course of the calculation. The difficulty associated with the boundary vorticity is a familiar one in fluid-dynamical calculations of this kind, and the technique adopted for its resolution is described in the summary below.

The second deficiency in the set of conditions is much more unusual. The A.D.I. method employed to find the temperature at grid points throughout the interior of the region of integration requires prior knowledge of the temperature at the centre of the vessel. A subsidiary calculation to obtain estimates of the centre temperature from equation (20), using previous iterates for the values of ϕ at neighbouring grid points, is incorporated into the overall iterative procedure.

We can now summarize the main steps of the numerical solution procedure employed to advance the solutions from, say, t_n to t_{n+1}. Values of the temperature ϕ at the ith mesh point in the r-direction and the jth mesh point in the θ-direction at time t_n are denoted by $\phi_{i,j,n}$ and similar notation is used for values of the other field variables. The steps in the iterative procedure are as follows:

(a) Using the current iterates for $\psi_{i,j,n+\frac{1}{2}}$ (or during the first iteration, values of $\psi_{i,j,n}$), the known values $\phi_{i,j,n}$ and an estimate of the temperature at the centre at time $t_{n+\frac{1}{2}}$ the first half step of the A.D.I. method is applied to equation (20) and the boundary conditions (14) and (23) to yield values for $\phi_{i,j,n+\frac{1}{2}}$ at all points except the centre.

(b) Values of $\omega_{i,j,n+\frac{1}{2}}$ are similarly obtained from equation (19) and the boundary condition (22) at all points except those on the outer boundary $r = 1$. The values at these points are required as boundary conditions for the A.D.I. method. The current iterates calculated in step (g) of the previous iteration are utilised, except during the first iteration, when the values at t_n are employed.

(c) The time-step for equation (20) begun in (a) is completed to yield $\phi_{i,j,n+1}$ except at the centre.

(d) Similarly, the time-step for (19) begun in (b) is completed, yielding $\omega_{i,j,n+1}$ except on $r = 1$.

(e) If $\chi^{(s)}$ denotes the values of $\phi_{i,j,n+1}$ found in (c), or of $\omega_{i,j,n+1}$ found in (d) during the current iteration, and $\chi^{(s-1)}$ the corresponding values in the preceding iteration, then $\chi^{(s)}$ is replaced by the weighted value defined by

$$\sigma\chi^{(s)} + (1 - \sigma)\chi^{(s-1)}, \tag{24}$$

where $0{\cdot}75 \leqslant \sigma \leqslant 0{\cdot}95$. This step was found to be essential for the convergence of the iteration procedure.

(f) The right-hand side of equation (18) is evaluated using the values $\omega_{i,j,n+1}$ thus obtained, and the equation is then solved by point over-relaxation to yield values $\psi_{i,j,n+1}$ at interior mesh points. The streamfunction is, of course, known to satisfy $\psi = 0$ for all times on the boundary of the region of integration by equations (21) and (22). The optimum value of the over-relaxation parameter λ was here found to lie in the range $1{\cdot}70 < \lambda < 1{\cdot}78$. The values of $\psi_{i,j,n+\frac{1}{2}}$ required in steps (a) and (b) may now be estimated from $\psi_{i,j,n}$ and $\psi_{i,j,n+1}$.

(g) The vorticity $\omega_{M,j,n+1}$, that is at points on the solid outer boundary $r = 1$, is calculated from the central-difference analogue of (18) applicable there, namely

$$\omega_{M,j,n+1} = -2\psi_{M-1,j,n+1}/(\delta r)^2 \tag{25}$$

where δr is the radial mesh size. Smoothing of these boundary vorticity values as in (24) was also necessary. The values $\omega_{M,j,n+\frac{1}{2}}$ required in (b) may now be estimated from $\omega_{M,j,n}$ and $\omega_{M,j,n+1}$.

(h) Values of the temperature at the centre at times $t_{n+\frac{1}{2}}$ and t_n required in steps (a)–(d) are found by incorporating the values of $\phi_{i,j,n+\frac{1}{2}}$ obtained in (a) and of $\phi_{i,j,n+1}$ obtained from (c) and (e) in the finite-difference analogue of (20) at the centre. During the first iteration, before new estimates may be found in this way, the centre temperature at time t_n is employed.

(i) The iteration cycle is repeated, beginning at step (a) until the maxima of the differences at each mesh

point between successive iterates for each of the fields ϕ, ψ and ω are less than prescribed tolerances. In the present work these were chosen to give nominally at least three significant figures in the solutions.

Steps (b) and (d) involve implicit linearisations of (19) since ω and ψ are there regarded as independent, though they are related by equation (18). The final non-linear term in (20) was treated by means of the following quasi-linearisation in the iterative procedure. At the sth stage, when $\phi^{(s-1)}$ was known and $\phi^{(s)}$ was being sought, the expression

$$e^{\phi^{(s)}} \simeq e^{\phi^{(s-1)}}[1 + (\phi^{(s)} - \phi^{(s-1)}], \qquad (26)$$

which is correct to second order in $(\phi^{(s)} - \phi^{(s-1)})$ was employed, since here β was taken to be zero. In practice this process and that associated with the centre temperature were found to converge somewhat more rapidly than that resulting from the implicit linearisation of equation (19). In other words, the temperature ϕ converges to its final value at each time-step more rapidly than do ω and ψ.

In the calculations described above, the spatial finite-difference mesh had 15 divisions in the r-direction and 20 in the θ-direction. The calculations were commenced using a time-step of 0·0025, but this was very quickly increased to 0·01 and eventually to 0·05 as steady-state solutions were approached. The extra computational effort required to include difference corrections in the present calculations was felt to be unjustified, since a comparison of the results obtained using the above mesh and those obtained for selected cases with the mesh lengths halved suggests that the principal features of the results would not be affected by more than about 5 per cent by their inclusion.

Calculations were performed for various combinations of parameters in the ranges $0 \leqslant Ra \leqslant 1{\cdot}1 \times 10^4$ and $2{\cdot}0 \leqslant \delta \leqslant 5{\cdot}0$. The lowest value of δ considered was thus the critical value for the onset of explosion when $\beta = 0$ according to Frank-Kamenetskii's purely conductive theory. The Prandtl number was taken to be unity throughout, a value representative of the reacting gas mixtures often used in experimental systems. (See note added in proof.) As indicated in Section 2, β was set equal to zero.

4. RESULTS AND DISCUSSION

One of the principal aims of this investigation is to determine the dependence on the Rayleigh number of the critical value δ_{CR} of Frank-Kamenetskii's parameter δ. This was achieved by performing the integration procedure described in Section 3 for a large number of combinations of values of δ and Ra and noting the nature of the resulting solutions. As described in Section 1, an explosion ensues when a net accumulation of heat in the system takes place as a result of heat being produced at a greater rate by the chemical reaction than that at which it can be removed by conduction through the walls of the vessel. The Arrhenian heat source term (1) in our model reflects the self-heating properties of systems in which an exothermic chemical reaction occurs; as the temperature T increases, the rate of production of heat increases rapidly and this may give rise to a self-accelerating process of heat production terminating in an explosion if the heat transfer processes are unable to remove the heat sufficiently quickly. Once an upward inflexion in the temperature versus time curve has occurred it is observed that an explosion does indeed always follow. When there is no such inflexion, the system proceeds to a steady state. Thus we have a criterion which allows us to divide the δ–Ra plane into two regions, corresponding to explosive and steady-state regimes. The critical curve separating the two regions which is obtained when the initial conditions (13) are given by

$$\phi_{INIT} = -0{\cdot}1 \cos(\pi r/2) \quad \text{and} \quad u_{INIT} = 0, \qquad (27)$$

is shown in Fig. 2.

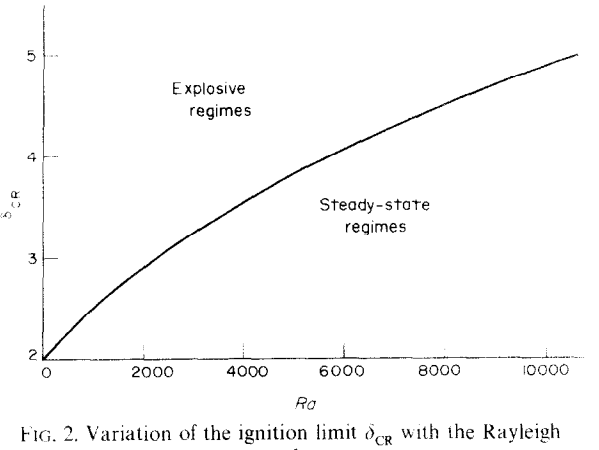

FIG. 2. Variation of the ignition limit δ_{CR} with the Rayleigh number.

It is clear that major modifications of the results of the classical theory may be required when account is taken of convective effects. If convection occurs in addition to conduction, the transfer of heat through the gaseous medium to the walls is improved, and thus larger values of δ, corresponding to higher rates of heat production by the reaction, may be accommodated without explosion. Since Rayleigh numbers of 2000 or more may easily be achieved in experimental situations, we see from Fig. 2 that the critical

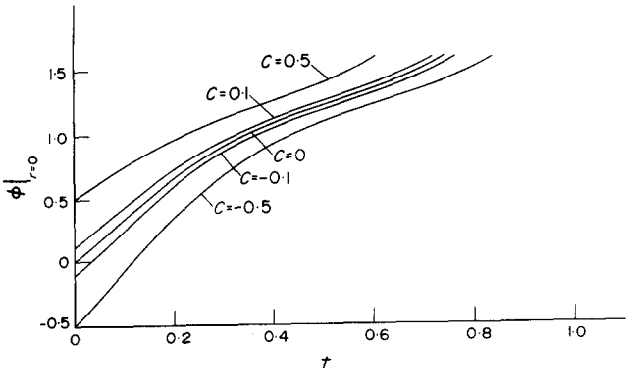

FIG. 3. Variation of the centre temperature with time when $\delta = 3{\cdot}0$ and $Ra = 10^3$. Initial conditions of the form (28) with values of C shown.

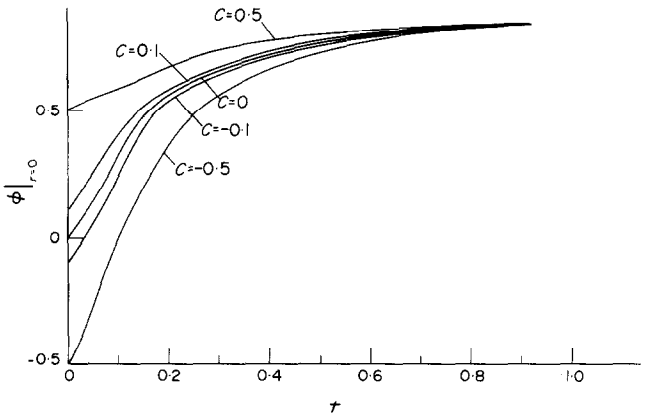

FIG. 4. Variation of the centre temperature with time when $\delta = 3{\cdot}0$ and $Ra = 4 \times 10^3$. Initial conditions of the form (28) with values of C shown.

values of δ encountered may well exceed the Frank-Kamenetskii value by over 50 per cent. The values of $\delta_{CR}(Ra)$ shown in Fig. 2 have been determined to within less than 10 per cent, which is sufficiently accurate for the purposes of comparison with experimental observations. There is no reason why in principle the critical conditions should not be determined much more accurately, but the computing time required to achieve this was felt to be prohibitive. The criterion for criticality used here is not, of course, the same as that employed by Frank-Kamenetskii, who sought the limiting value of δ for which solutions of the steady-state diffusion equation were available. However, when the Rayleigh number was set to zero in the present calculations, to correspond to the case of purely conductive heat transfer, the critical value obtained was 2·01, compared with Frank-Kamenetskii's value of 2·00.

The use of initial conditions other than those defined by (27) has negligible effect on the critical curve of Fig. 2, provided they are not sufficiently extreme to induce an explosion immediately. Naturally, however, the transient behaviour of the solutions will vary with the initial conditions chosen. This is illustrated in Fig. 3, where the variation of the temperature at the centre of the cylinder with time is plotted for a system in the explosive region, and in Fig. 4, in which the transient behaviour of a non-explosive regime is shown. In both cases the initial conditions imposed are of the form

$$\phi_{\text{INIT}} = C \cos(\pi r/2) \quad \text{and} \quad \boldsymbol{u}_{\text{INIT}} \equiv 0, \tag{28}$$

where C lies in the range $-0{\cdot}5 \leqslant c \leqslant 0{\cdot}5$. The integrations were terminated in explosive regimes when the integration procedure no longer converged for a time-step of length 0·01 and in steady-state regimes

when solutions at successive time-steps 0·05 apart differed by less than 0·5 per cent.

Figure 5 shows the development of the maximum temperature in the system with time, from initial conditions defined by

$$\phi_{\text{INIT}} = 0{\cdot}1 \cos(\pi r/2) \quad \text{and} \quad \boldsymbol{u}_{\text{INIT}} \equiv 0, \tag{29}$$

for several values of the Rayleigh number, some too small to prevent an explosion at the given value of δ, and some sufficiently large to allow a steady-state regime to be attained. The greatest steady maximum

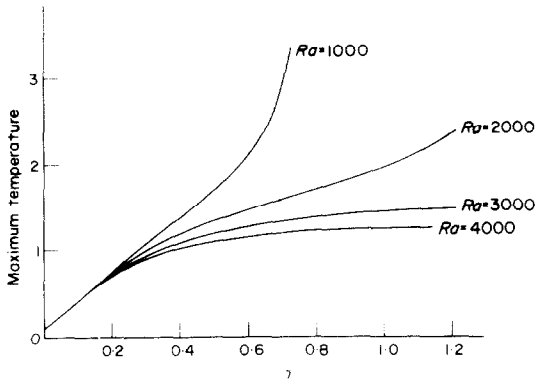

FIG. 5. Variation of the maximum temperature with time when $\delta = 3{\cdot}0$ at the values of Ra shown. Initial conditions of the form (29).

temperature approached in the steady-state regimes is larger than that, $\phi = 1{\cdot}37$, predicted by the purely conductive theory. This reflects the possibility, when convection occurs, of steady-state regimes for values of δ exceeding the critical value of the classical theory. This is confirmed by the observations of Archer and Tyler [10].

More details of the development of the temperature field in one of the cases ($Ra = 4000$) represented in Fig. 5 are shown in the sequence of temperature profiles across the vertical diameter displayed in Fig. 6. The temperature within the vessel increases steadily with time and the maximum moves up from its initial central position accompanying an upwelling of hot gas in the centre of the vessel. A similar displacement of the temperature maximum has been observed in [4] and [5].

When the initial conditions (29) are replaced by (27) the transient behaviour is much more complicated. This is illustrated by the temperature profiles shown in Fig. 7 and in the temperature and stream function distributions of Fig. 8. Initially heat is absorbed from the surroundings. Nonetheless, it is mainly as a result of the fact that the rate of heat generation by the reaction is a strongly increasing function of temperature that temperature maxima are quickly established close to the walls of the vessel. Consequently, the reacting gas rises in the relatively warm layers near to the walls and falls near the centre of the cylinder, where the gas is cooler. This accounts for the temperature and stream function distributions shown in Fig. 8(i). As more heat is released by the reaction the temperature maxima move inwards, so that the region near the centre of the vessel and the layers near the walls are both cooler than the intervening region. Then the warmer fluid in the intermediate region rises whilst the cooler fluid near the walls and in the centre of the vessel falls, leading to the double circulation pattern shown in Fig. 8(b)(ii). The outer circulation grows at the expense of the inner flow as the accumulation of heat produced by the reaction near the centre causes the temperature there

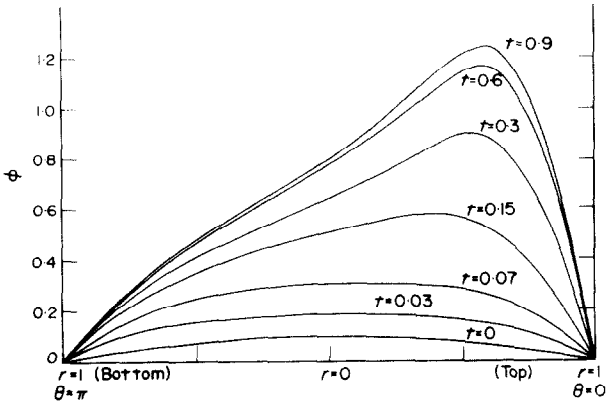

FIG. 6. Temperature profiles across the vertical diameter at the times shown when $\delta = 3{\cdot}0$ and $Ra = 4 \times 10^3$. Initial conditions of the form (29).

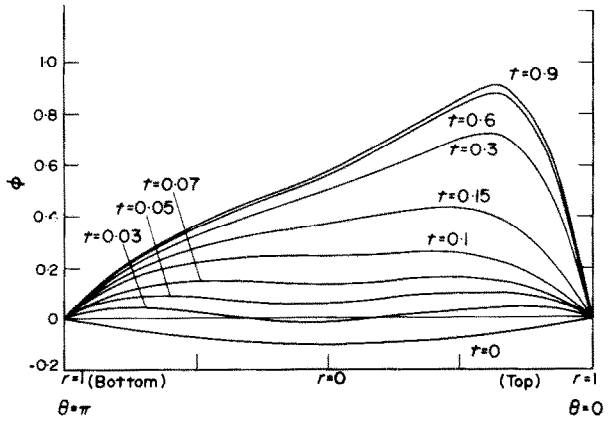

FIG. 7. Temperature profiles across the vertical diameter at the times shown when $\delta = 3{\cdot}0$ and $Ra = 10^4$. Initial conditions of the form (27).

to rise. Eventually the entire semicircular region is occupied by the steady-state circulation, with an upwelling of hot fluid in the centre of the vessel and cooler fluid falling near the walls. A similar development of the velocity field takes place when the system is in an explosive regime but then heat is produced more rapidly in the centre of the vessel than it can be removed by the combined conduction and convection processes.

There is excellent qualitative agreement between the results presented here for a cylindrical geometry and the observations made by Archer and Tyler [10]

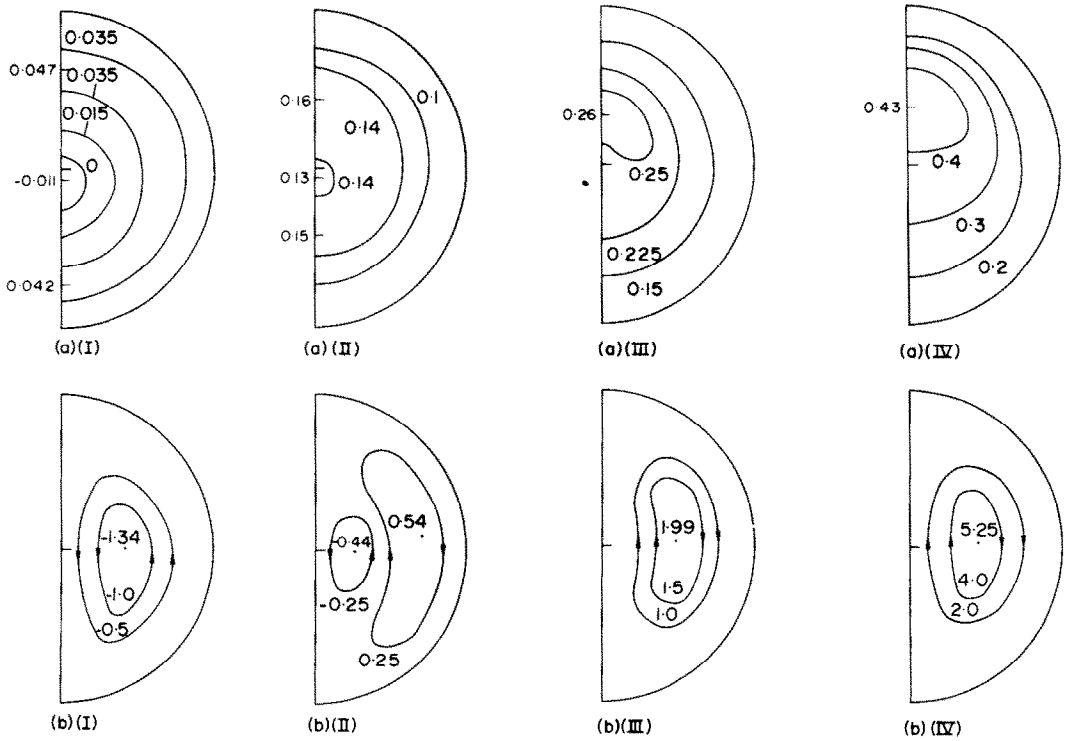

FIG. 8. (a) Temperature distributions and (b) streamfunction distributions when $\delta = 3{\cdot}0$ and $Ra = 10^4$ at times (i) 0·03 (ii) 0·07 (iii) 0·1 (iv) 0·15 (v) 0·3. Initial conditions of the form (27).

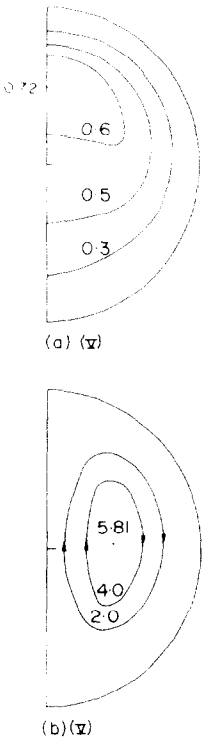

of experiments in spherical apparatus. The initial conditions defined by

$$\phi_{\text{INIT}} = -0{\cdot}5\cos(\pi r/2) \quad \text{and} \quad \boldsymbol{u}_{\text{INIT}} \equiv 0, \tag{30}$$

correspond most closely to those of the experimental situation although there the initial temperature distribution is not symmetrical about the centre of the vessel, and some swirling motion of the reacting gaseous mixture accompanies its introduction into the vessel, so that the condition $\boldsymbol{u}_{\text{INIT}} \equiv 0$ applied here will not be appropriate. It is anticipated that the main features of integrations in a spherical geometry will be similar to those for the cylindrical geometry described here. It is hoped that more extensive calculations will allow quantitative comparisons with the experimental results to be made and reported later.

5. CONCLUSION

Despite the limitations of the model adopted, such as those arising from the use of the Boussinesq approximation, which may be expected to become less appropriate as large temperature rises are encountered in explosive regimes, from the symmetry assumptions and from the forms of the initial conditions, it may safely be asserted that the modifications of the predictions of the classical theory demanded by the inclusion of convective processes are considerably greater than those arising from the incorporation of reactant consumption or from a consideration of non-zero values of the parameter β. Earlier calculations (see [3] and [9]) using parameter values typical of experimental situations have shown that each of the latter modifications leads to enhancements of the critical δ values of about 5 per cent at most. In contrast, the present calculations suggest that even at moderate Rayleigh numbers such as 2000, the critical value of δ may be increased by about 50 per cent, whilst at Rayleigh numbers $0(10^4)$, which are still attainable in experimental systems, the increase may be of 200–300 per cent.

Acknowledgements—The author wishes to express his thanks to Professor N. Riley for his helpful supervision of this work, to Mrs. W. H. Archer and Dr. B. J. Tyler for useful discussions, and to the Science Research Council for financial support.

REFERENCES

1. D. A. Frank-Kamenetskii, *Diffusion and Heat Exchange in Chemical Kinetics* (translated by N. Thon). Chapters VI and VII. Princeton University Press, Princeton (1955).
2. V. V. Barzykin, V. T. Gontkovskaya, A. G. Merzhanov and S. I. Khudyaev, A theory of thermal explosions in the unsteady state, *J. Appl. Mech. Tech. Phys.* 196–209 (1964), translated from *Zh. Prikl. Mekhan. i Tekhn. Fiz.*
3. B. J. Tyler and T. A. B. Wesley, Numerical calculations of the critical conditions in thermal explosion theory with reactant consumption, Eleventh Symposium (International) on Combustion, pp. 1115–1122. The Combustion Institute, Pittsburgh, Pennsylvania (1967).
4. B. J. Tyler, An experimental investigation of conductive and convective heat transfer during exothermic gas phase reactions, *Combust. Flame* **10**, 90–91 (1966).
5. P. G. Ashmore, B. J. Tyler and T. A. B. Wesley, Experimental investigations of conductive and convective heat transfer in relation to thermal ignitions, Eleventh Symposium (International) on Combustion, pp. 1133–1140. The Combustion Institute, Pittsburgh, Pennsylvania (1967).
6. A. G. Merzhanov and É. A. Shtessel, Thermal explosions in a liquid state exposed to natural convection, *Dokl. Phys. Chem.* **194**, 671–674 (1970); translated from *Dokl. Akad. Nauk. SSSR (Phys. Chem.)*.
7. D. R. Jones, The dynamic stability of confined, exothermically reacting fluids, *Int. J. Heat Mass Transfer* **16**, 157–167 (1973).
8. D. W. Peaceman and H. H. Rachford, The numerical solution of parabolic elliptic differential equations, *J. Soc. Ind. Appl. Math.* **3**, 28–41 (1955).
9. J. R. Parks, Criticality criteria for various configurations of a self-heating chemical as a function of activation energy and temperature of assembly, *J. Chem. Phys.* **34**, 46–50 (1961).
10. W. H. Archer and B. J. Tyler, Private communication (1972).

NOTE ADDED IN PROOF

The results of calculations with $Pr = 20$ reported by V. V. Barzykin, A. G. Merzhanov, F. I. Dubovitsky, E. A. Shtessel and A. S. Shteinberg (Thermal explosion of explosives in the liquid phase, 2nd Symposium on Chemical Problems connected with the Stability of Explosives, Tyringe, Sweden, 1970) are in broad agreement with those for $Pr = 1$ presented here.

EFFETS DE CONVECTION DANS DES GAZ EN REACTION EXOTHERMIQUE DANS UNE ENCEINTE

Résumé—Par intégration numérique des équations gouvernant la dynamique des fluides on met en évidence les conséquences de la convection qui apparait dans le cas de réactions chimiques exothermiques en milieu gazeux confiné dans un cylindre circulaire horizontal. Les effets thermiques de la réaction sont représentés par une distribution de sources de chaleur avec une dépendance vis à vis de la température selon la loi d'Arrenius, mais on ne tient pas compte de la consommation des réactants. La limite d'ignition δ_{cr} est une fonction fortement croissante du nombre de Rayleigh et les distributions de température dans l'enceinte ne sont pas longtemps symétriques quand apparait la convection. On obtient un bon accord qualitatif avec les effets convectifs observés dans des expériences faites avec d'autres géométries d'enceinte.

KONVEKTIONSEFFEKTE IN EINEM EINGESCHLOSSENEN, EXOTHERM REAGIERENDEN GAS

Zusammenfassung—Durch numerische Integration der bestimmenden hydrodynamischen Gleichungen mittels einer A.D.I.-Methode werden die Auswirkungen des Auftretens von Konvektion bei der exothermen chemischen Reaktion in einem gasförmigen Medium, das in einem horizontalen kreisförmigen Zylinder eingeschlossen ist, untersucht. Die thermischen Effekte der Reaktion werden durch eine Verteilung von Wärmequellen mit Arrheniustemperaturabhängigkeit dargestellt.

Der Verbrauch an Reaktanten während der Reaktion wird vernachlässigt. Die Zündgrenze δ_{CR} steigt mit der Rayleigh-Zahl stark an und die Temperaturverteilungen in dem Gefäss sind nicht mehr symmetrisch zum Zentrum, wenn Konvektion auftritt. Mit Experimenten, die andere Gefässgeometrien verwendeten, besteht bei der Betrachtung der Konvektionseffekte gute qualitative Übereinstimmung.

КОНВЕКЦИЯ В ГАЗАХ, ЗАКЛЮЧЕННЫХ В СОСУД, ПРИ НАЛИЧИИ ЭКЗОТЕРМИЧЕСКОЙ РЕАКЦИИ

Аннотация—С помощью численного интегрирования основных газодинамических уравнений проведено исследование влияния конвекции в газовой среде, заключенной в горизонтальный круговой цилиндр, при наличии экзотермических химических реакций. Тепловые эффекты реакции представлены распределением источников тепла при температурной зависимости Аррениуса, а расходом реагентов во время реакции пренебрегается. Установлено, что предел воспламенения δ_{cr} является быстро возрастающей функцией числа Релея, а распределения температуры в сосуде при наличии конвекции перестают быть симметричными относительно центра. Получено хорошее качественное соответствие с результатами экспериментов по свободной конвекции в сосудах иной формы.